Relapse-associated AURKB blunts the glucocorticoid sensitivity of B cell acute lymphoblastic leukemia

Coralie Poulard[a], Hye Na Kim[b,c,1], Mimi Fang[d,1], Karina Kruth[d], Celine Gagnieux[a], Daniel S. Gerke[a], Deepa Bhojwani[b,c], Yong-Mi Kim[b,c], Martin Kampmann[e,f], Michael R. Stallcup[a,2], and Miles A. Pufall[d,2]

[a]Department of Biochemistry and Molecular Medicine, Norris Comprehensive Cancer Center, University of Southern California, Los Angeles, CA 90089; [b]Department of Pediatrics, Division of Hematology, Oncology, and Bone Marrow Transplantation, Children's Hospital Los Angeles, Los Angeles, CA 90027; [c]Department of Pediatrics, Keck School of Medicine, University of Southern California, Los Angeles, CA 90033; [d]Department of Biochemistry, Holden Comprehensive Cancer Center, Carver College of Medicine, University of Iowa, Iowa City, IA 52242; [e]Institute for Neurodegenerative Diseases, Department of Biochemistry and Biophysics, University of California, San Francisco, CA 94158; and [f]Chan Zuckerberg Biohub, San Francisco, CA 94158

Edited by Keith R. Yamamoto, University of California, San Francisco, CA, and approved January 3, 2019 (received for review September 19, 2018)

Glucocorticoids (GCs) are used in combination chemotherapies as front-line treatment for B cell acute lymphoblastic leukemia (B-ALL). Although effective, many patients relapse and become resistant to chemotherapy and GCs in particular. Why these patients relapse is not clear. We took a comprehensive, functional genomics approach to identify sources of GC resistance. A genome-wide shRNA screen identified the transcriptional coactivators EHMT2, EHMT1, and CBX3 as important contributors to GC-induced cell death. This complex selectively supports GC-induced expression of genes contributing to cell death. A metaanalysis of gene expression data from B-ALL patient specimens revealed that Aurora kinase B (AURKB), which restrains GC signaling by phosphorylating EHMT1-2, is overexpressed in relapsed B-ALL, suggesting it as a potential contributor to relapse. Inhibition of AURKB enhanced GC-induced expression of cell death genes, resulting in potentiation of GC cytotoxicity in cell lines and relapsed B-ALL patient samples. This function for AURKB is distinct from its canonical role in the cell cycle. These results show the utility of functional genomics in understanding mechanisms of resistance and rapidly identifying combination chemotherapeutics.

glucocorticoid | leukemia | coregulator | AURKB | cell death

Glucocorticoids (GCs), including dexamethasone (dex) and prednisone, are a component of front-line combination chemotherapy used to treat lymphoid cancers (1). In children with B cell acute lymphoblastic leukemia (B-ALL), overall treatment response is correlated with response to GCs alone, indicating that GCs are a key component in treatment efficacy (2–4). GCs work by binding to the glucocorticoid receptor (GR), a ligand-activated transcription factor that then translocates to the nucleus, associates with DNA, and regulates genes (5). Regulation of genes by GR is essential to the cytotoxicity of GCs (6). Although effective, about 15% of children with B-ALL do not respond to GC-based combination chemotherapy or develop resistance on relapse (7). Despite remarkable advances in immunotherapy, the prognosis of these patients remains poor (8), underscoring the immediate need for new treatments.

One strategy to improve treatment of patients with relapsed B-ALL is to understand the mechanism of relapse and GC resistance specifically. One route to relapse is mutation. We previously demonstrated that mutations associated with resistance or relapse are in genes that modulate the sensitivity of B-ALL to GCs (9). Among these, transcription factors and GR coregulators [e.g., *CREBBP*/*P300* and *TBL1XR1* (10)] are prevalent (11), underscoring their importance as potential therapeutic targets. Despite these findings, genetic lesions explain only a small fraction of GC resistance (12).

Another potential source of resistance to GCs is gene misexpression. Studies comparing the gene expression of patients at diagnosis with that at relapse in children with B-ALL identify dozens of significantly misexpressed genes that were most prominently related to cell cycle and replication (e.g., *PTTG1*, *CDC20*), apoptosis (*BIRC5*, *HRK*), and DNA repair (*FANC* genes) (13–15). Integration of misexpression with other data, including DNA methylation and copy number variation, yielded higher-confidence hits, including in cell cycle, WNT, and MAPK pathways (14). Nonetheless, few functional links between gene misexpression and GC resistance have been established, thwarting development of therapies to overcome resistance.

Recently, we took a functional genomic approach to identify targets for potentiating GCs specifically in the tissue of interest. By integrating the response of B-ALL samples to GCs with an shRNA screen encompassing one-quarter of the genome (~5,600 genes), we identified a previously obscured role for GCs in regulating B cell developmental programs (9). Inhibiting a node in the B cell receptor signaling network, the lymphoid-restricted PI3Kδ, potentiated GCs even in some resistant patient samples (9). Although this combination would be expected to have few side effects, it does not specifically target sources of relapse that would attenuate GC function.

In this study, we took a comprehensive functional genomic approach to understanding how GCs induce cell death in B-ALL

Significance

Understanding the mechanism of glucocorticoid-induced cell death and resistance on relapse is essential to improve treatment of leukemias. We used functional genomics, integrating gene regulation, gene misexpression on relapse, and genome-wide shRNA screen in B cell acute lymphoblastic leukemia (B-ALL). This revealed that glucocorticoids deploy select transcriptional cofactors to regulate effector genes that drive, and buffer genes that restrain, cell death. Aurora kinase B (AURKB), a negative regulator of the EHMT1/2 coregulator complex, was found to be overexpressed on relapse. Inhibitors of AURKB enhanced glucocorticoid regulation of effector genes while leaving key buffering genes unperturbed, resulting in potentiated glucocorticoid sensitivity in B-ALL cell lines and relapsed patient samples. This provides a potential therapy and deeper understanding of glucocorticoids in leukemia.

Author contributions: C.P., H.N.K., K.K., D.B., Y.-M.K., M.K., M.R.S., and M.A.P. designed research; C.P., H.N.K., M.F., K.K., C.G., and D.S.G. performed research; C.P., H.N.K., K.K., and M.A.P. analyzed data; and C.P., M.R.S., and M.A.P. wrote the paper.

The authors declare no conflict of interest.

This article is a PNAS Direct Submission.

Data deposition: Normalized intensity values from the Illumina HT12 v4 arrays used to analyze the effect of coregulator depletion on dex-regulated gene expression have been deposited in the Gene Expression Omnibus (accession no. GSE118992).

[1]H.N.K. and M.F. contributed equally to this work.

[2]To whom correspondence may be addressed. Email: stallcup@usc.edu or miles-pufall@uiowa.edu.

This article contains supporting information online at www.pnas.org/lookup/suppl/doi:10.1073/pnas.1816254116/-/DCSupplemental.

and to identify sources of GC resistance. Results of a genome-wide shRNA screen (>20,000 protein coding genes) were integrated with data for dex regulation of gene expression to identify genes that contribute to dex-induced cell death. Screen results were then combined with an integrated analysis of available datasets of gene expression at diagnosis and relapse in children with B-ALL to identify misexpressed genes that affect growth and sensitivity. This approach identified numerous potential targets, such as cell cycle and transcriptional regulatory complexes. In particular, a specific GR transcriptional coactivator complex [EHMT1 (also known as GLP), EHMT2 (also known as G9a), and CBX3 (also known as HP1γ)] was implicated as a required component for efficient GC-induced cell death. We found that a negative regulator of the complex, Aurora kinase B (AURKB) (16), is overexpressed in relapsed B-ALL, implicating it as a source of resistance. Adding AURKB inhibitors increased GC-induced cell death of B-ALL at least in part by enhancing the activity of the EHMT2 and EHMT1 working with GR.

Results

Genome-Wide Identification of Genes That Influence Sensitivity to GC-Induced Cell Death. To determine the contribution of each gene in the genome to cell growth and GC-induced cell death in B-ALL, we used a next generation shRNA screen (9, 17). We performed this screen in NALM6 cells, which we demonstrated

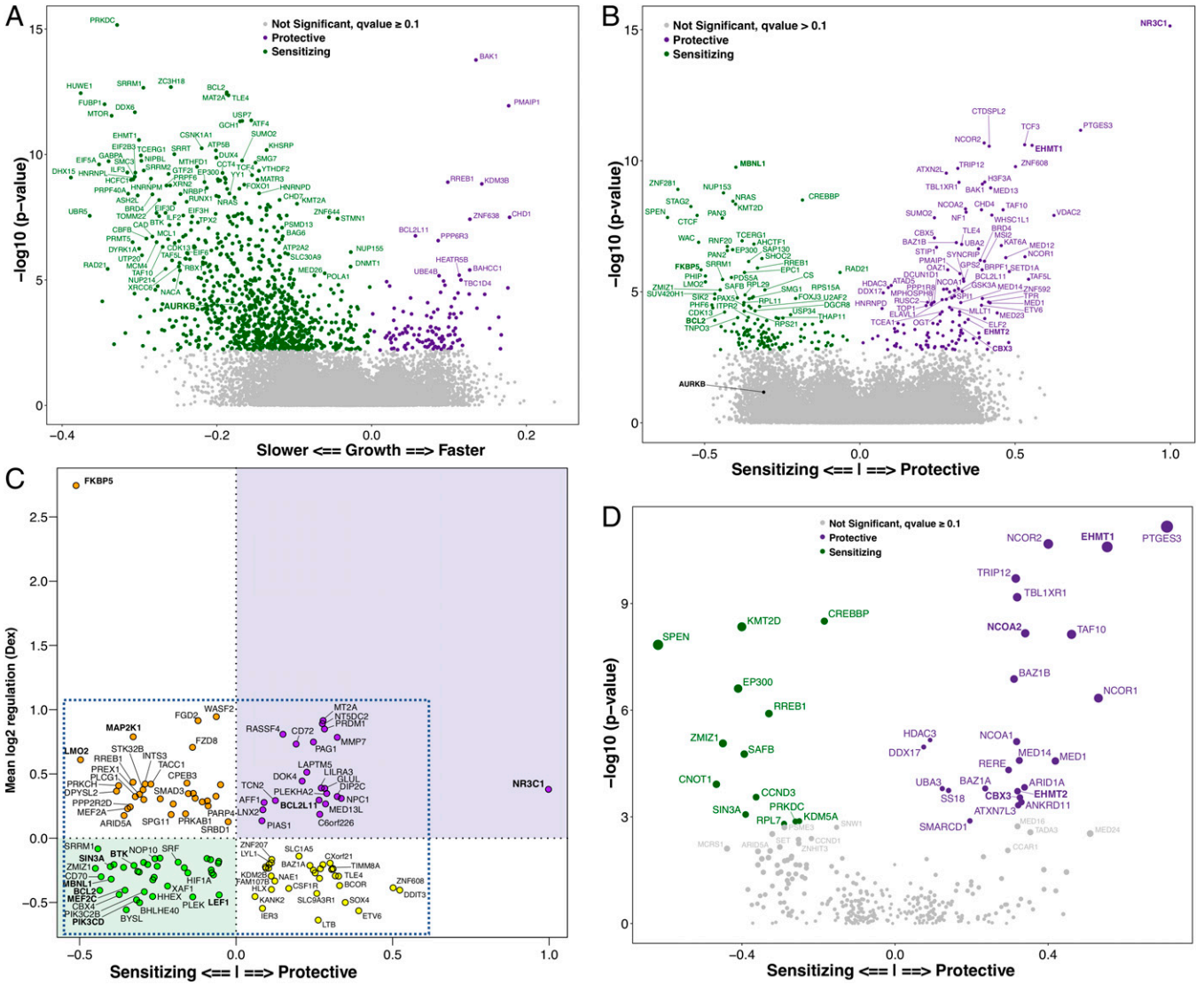

Fig. 1. Genes that affect growth and sensitivity to dex in the B-ALL cell line NALM6. (*A*) Growth or γ values are calculated by averaging enrichment of each shRNA in the cell population at the end of the growth period (TF) vs. at initial infection (T0) (*SI Appendix, SI Methods*). Confidence values (*P* values) are calculated by MW test comparing enrichment of shRNAs vs. thousands of control shRNAs. Points are colored if the genes significantly (q value ≤ 0.1) decrease (green) or increase (purple) growth on depletion. (*B*) ρ or dex sensitivity values are calculated for each gene as effect of depletion on average enrichment of shRNAs on dex treatment (R1–R3) vs. growth control (TF) (*SI Appendix, SI Methods*). Confidence values (*P* values) are calculated by MW test comparing enrichment of shRNAs vs. thousands of control shRNAs. Green points, genes that sensitize cells to dex when depleted; purple points, those that render cells more resistant when depleted. (*C*) Effector plot for genes that effect dex-induced cell death. From genes with a significant (*P* value ≤ 0.05) effect on dex-induced cell death (*B* and Dataset S1), a subset was identified that overlaps with the set of genes consistently and significantly regulated (KS test; q value ≤ 1e-3) by GCs in B-ALL primary samples, patient-derived xenografts, and cell lines (9). These genes are plotted by effect of depletion on cell death (1, perfectly protective; −1, twofold increase in sensitivity) vs. average regulation in response to dex. Genes with up-regulation (purple) or repression (green) by dex that contributes to dex-induced cell death are effectors. Genes with up-regulation (orange) or repression (yellow) that opposes cell death are buffering genes (refer to *SI Appendix*, Fig. S2). (*D*) Volcano plot depicts the effect of depletion on dex sensitivity for all known nuclear receptor coregulators (points are a subset of *B*).

previously to be a useful cell line model for the response of patient specimens and patient-derived xenograft samples to GCs (9). We targeted each known protein coding gene (~20,000) with an average of 25 shRNAs delivered by lentivirus. Starting with 6 billion cells, we performed the screen with three biological replicates as described previously, except in spinner flasks rather than still tissue culture flasks to accommodate the vastly greater number of genes screened (9, 18, 19). Infected cells were then treated three times with vehicle or 35 nM dex (~EC_{50}) for 3 d each time, washing the drug out in between. By comparing the enrichment of integrated shRNA expression cassettes in the vehicle vs. initially infected cells, we calculated the effect of each gene on growth (γ score). By comparing the enrichment in cells treated with dex vs. vehicle, we calculated the effect on dex sensitivity (ρ score). The dex sensitivity scores were highly consistent between biological repeats (*SI Appendix*, Fig. S1*A* and *SI Methods* has details). This design not only identified high-confidence hits but also, identified genes that both contribute to and restrain the response of cells to GCs (17, 18, 20).

Hundreds of genes significantly affected growth (γ scores). Significance was calculated by Mann–Whitney *U* (MW) and Kolmogorov–Smirnov (KS) tests, which generally agreed well, except for a cohort of genes that exhibited greater significance by MW (*SI Appendix*, Fig. S1*B*). This is likely because shRNAs that affect growth severely dropped out of the screen, and the MW test is less sensitive to a smaller number of shRNAs. Nonetheless, ~5% of genes (1,030, q value ≤ 0.1) (21) affected growth, with the majority (910 genes) impeding growth when depleted (Fig. 1*A*, Dataset S1, and *SI Appendix*, Fig. S1*C*). Depletion of components involved in translation, mammalian target of rapamycin (mTOR) signaling, and energy production had a negative impact on growth (*SI Appendix*, Fig. S1*D*). The B cell receptor pathway was also important, likely because signaling through this pathway enhances growth and survival of NALM6 cells (9). AURKB, an important mitosis facilitator that proved to be highly relevant to this study, was also a significant contributor to cell growth.

Hundreds of genes were also found to affect dex sensitivity (ρ scores). The 276 most significant genes (q value ≤ 0.1) were split between those that contribute to GC-induced cell death (130; protective on knockdown) (Fig. 1*B*, purple) and those that attenuate the toxicity of dex (146; sensitizing on knockdown) (Fig. 1*B*, green). Importantly, depletion of GR (*NR3C1*) was the most protective, highest-confidence hit in the screen. At the other end of the spectrum, MBNL1 was the most significant sensitizing hit. Sensitizing hits are of immediate therapeutic interest, as inhibitors of these proteins are good candidates for sensitizing cells to dex. Similar to γ, the MW and KS tests for ρ scores were consistent but did not agree for a cohort of genes, again likely because of shRNA dropout during dex treatment (*SI Appendix*, Fig. S1*E*). This dropout likely caused an underestimation of the significance of some genes (false negatives) but would not diminish the confidence of significant hits. For example, five *AURKB* shRNAs dropped out after dex treatment, presumably because they rendered cells extremely sensitive to dex. This resulted in apparently marginal significance (*P* value = 0.15), despite a substantial phenotype value (ρ = −0.30) (*SI Appendix*, Fig. S1*F*). In subsequent analyses, we therefore use a q value ≤ 0.1 cutoff to identify significant genes and a more relaxed cutoff (*P* value ≤ 0.05) for pathway and exploratory data analyses (top genes).

Identification of GC-Regulated Cell Death Effector Genes. Previously, we identified genes that are consistently regulated by GCs in B-ALL by combining measured changes in gene expression with existing data for primary samples, patient-derived xenografts, and cell lines (9). Using a stringent cutoff (KS test; q value ≤ 1e-3), we found that 1,040 genes were regulated across dex-sensitive B-ALL samples, with about one-half being activated and one-half being repressed. By comparing the genes regulated by dex in B-ALL cells with the top hits from our shRNA screen, we identified GC-regulated genes that affect cell death (Dataset S2).

Effectors are genes with regulation by dex that contributes to cell death. If activation of a gene contributes to cell death, then depletion would make cells more resistant (Fig. 1*C* and *SI Appendix*, Fig. S2*A*, purple) or would increase cell growth (*SI Appendix*, Fig. S2 *B*, purple and *C*, purple). If repression contributes to cell death, then depletion would render the cells more sensitive to dex (Fig. 1*C* and *SI Appendix*, Fig. S2*A*, green) or would impede cell growth (*SI Appendix*, Fig. S2 *B*, green and *C*, green). In total, 60 genes were classified as effectors by their effect on dex sensitivity (ρ), and 108 genes were classified as effectors by their effect on growth (γ). These effectors include BH3 apoptosis family members (e.g., BCL2, BCL1L11), B cell receptor/PI3K pathway components (e.g., BTK, PIK3CD), and B cell development genes (e.g., LEF1, MEF2C). Two splicing factors, MBNL1, which is mutated in some leukemias (22–24), and SRRM1 (25), are strong, negative effectors, suggesting that GC regulation of splicing contributes to B-ALL death.

The full screen also revealed a number of genes that buffer dex efficacy. Buffering genes are genes with regulation that would counteract the cytotoxicity of GCs. These include genes that are up-regulated by dex and have depletion that renders cells more sensitive and genes that are repressed and have depletion that renders cells more resistant (Fig. 1*C* and *SI Appendix*, Fig. S2,

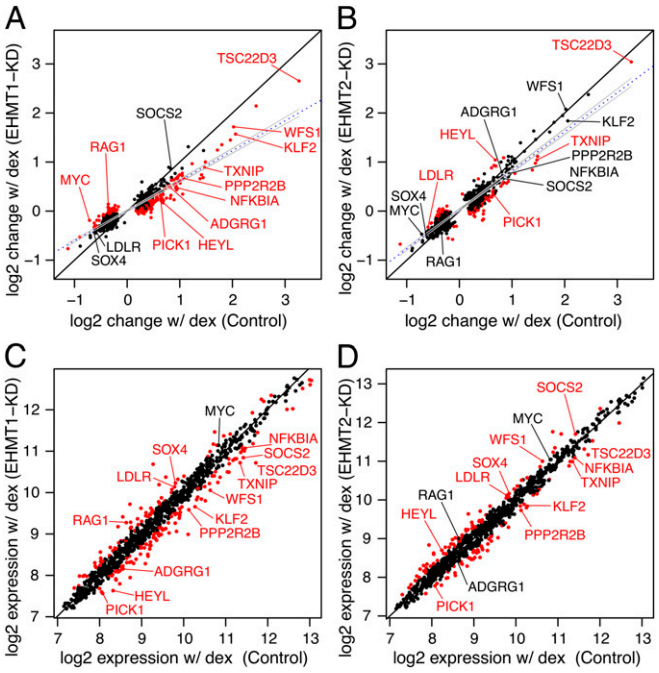

Fig. 2. Each coregulator supports GC regulation of a subset of GR target genes. EHMT1 (*A* and *C*) and EHMT2 (*B* and *D*) were knocked down and treated with dex for 4 h (three biological replicates), and total RNA was analyzed on Illumina microarrays. (*A* and *B*) Genes significantly regulated in control (scrambled shRNA) or knockdown in response to dex were plotted. Each point represents log2 change in expression after dex exposure for control (*x* axis) or knockdown (*y* axis) for each gene. The dotted lines represent the linear least squared regression fits to the points, and the flanking curved lines are 99% confidence intervals about that line. Red dots, genes that do not fit (*P* value ≤ 0.01) a slope of one (solid line), representing no change. (*C* and *D*) Expression levels in dex-treated cells for genes significantly regulated by dex under any condition are plotted for control (*x* axis) vs. knockdown (*y* axis). Lines of slopes of one (solid lines) representing no change in regulation are plotted for comparison. Genes significantly different (*P* value ≤ 0.01) are red. Genes referred to in the text are labeled.

orange and yellow points). The most prominent among the buffering genes is FKBP5, which is among the top three most dex-activated genes and strongly sensitizes cells when depleted. Buffering genes with a direct link to leukemia include PREX1 and MAP2K1 (MEK1), which activate RAS/MAPK pathways promoting survival (26), and LMO2, which is an oncogene in T cell acute lymphoblastic leukemia (27). These results indicate that GCs are not cleanly cytotoxic; instead, they regulate genes that oppose their own toxicity in B-ALL. These genes reflect the diverse biology of GCs, misregulation of which may be a source of resistance in some B-ALLs. This unexplored set of buffer genes is an excellent potential target for therapies, as inhibition would counteract the regulation of buffering genes, increasing the cytotoxicity of GCs.

Specific Nuclear Receptor Coregulators Affect Dex Sensitivity. Pathway analysis of the screen indicated that the estrogen and GC signaling pathways have a significant impact on GC-induced cell death (*SI Appendix*, Fig. S1*G*). Because knockdown of estrogen receptor (ER) itself did not have an effect (q value = 0.78), identification of the ER pathway is likely because ER and GR interact with many of the same coregulators and transcription factors.

Our results clearly indicate that nuclear receptor coregulators significantly affect GC sensitivity. Of the 337 proteins in this class identified online and compiled from the literature for this study (https://www.nursa.org/nursa/index.jsf) (28–30), about one-quarter (80) were among the top genes (P value ≤ 0.05) implicated in GC-induced cell death (Dataset S3), with 37 being highly significant (q value ≤ 0.1) (Fig. 1*D*). Depletion of 33 coregulators reduced sensitivity to dex (e.g., *PTGES3*, *EHMT1*), indicating that these coregulators contribute to GC-induced cell death. The most prominent hit was *PTGES3* (also known as p23), a chaperone that serves both as a coregulator for GR and as an enzyme producing the prostaglandin PGE2 (31). Depletion of the other 47 coregulators sensitized NALM6 cells to dex, including CREBBP, which is frequently mutated in cancers, KMT2D, and components of the NuRD complex (including HDAC2, MAT1, SPEN, MBD2/3, and GATAD2B) (32). This indicates that these cofactors attenuate GC-induced cell death and would be good targets for inhibitors to sensitize B-ALL. We, therefore, hypothesized that specific coregulators would cooperate with GR to regulate genes involved in GC-induced cell death.

Depletion of Coregulators Generally Attenuates Dex Regulation and Causes Misregulation of Specific GC-Regulated Genes. To understand mechanistically how coregulator depletion affects dex sensitivity, we measured the effect of depleting selected coregulators with shRNA on dex regulation of genes. We chose EHMT1 and EHMT2, two known GR coregulators, because (*i*) they have strong significant positive ρ scores (Fig. 1*D*) (EHMT1 had one of the top scores in the screen), (*ii*) EHMT2 is homologous to EHMT1 and heterodimerizes with it, and (*iii*) we have extensively characterized their mechanism of action with GR (16, 33, 34). We then treated three biological replicates of NALM6 cells and two controls (uninfected, scrambled shRNA) with dex or vehicle, measured gene expression by microarray (Illumina HT12 v4), and calculated differential gene expression (*lumi*/*limma*, R/Bioconductor) (Dataset S4).

Depletion of each coregulator resulted in fewer genes significantly regulated by dex (q value < 0.01) (*SI Appendix*, Fig. S3). Much of this effect is due to a general attenuation of dex regulation of genes, with depletion of each coregulator attenuating both activation and repression of genes compared with controls (Fig. 2 *A* and *B*). Depletion of EHMT1 had a more pronounced effect (average of 38% attenuation compared with ∼20% for EHMT2), likely because of a concomitant reduction in EHMT2 protein level (35). The majority of genes seems to fit this trend ($r^2 = 0.86$–0.88), but other genes exhibited a more significant change in regulation (Fig. 2 *A*, red dots and *B*, red dots). Some cell death effector genes did not follow this trend (*MEF2C*, *LEF1*, *ZMIZ1*) and seemed to be unaffected by cofactor depletion. Other effector genes are reliant on a specific coregulator (EHMT1), including *MYC* and *RAG1* (9). Thus, these coregulators have both general and specific effects on dex regulation of genes that contribute to B-ALL cell death.

Separate from an effect on regulation by dex, coregulator depletion also significantly changed mRNA levels of some genes in the presence of dex. This is important, because the ultimate expression level of a gene on addition of dex governs the biological response rather than the fold change. Comparing the mRNA levels of dex-treated control cells with coregulator-depleted cells (Fig. 2 *C* and *D*), 468 (EHMT1-KD) and 305 (EMHT2-KD) genes exhibited

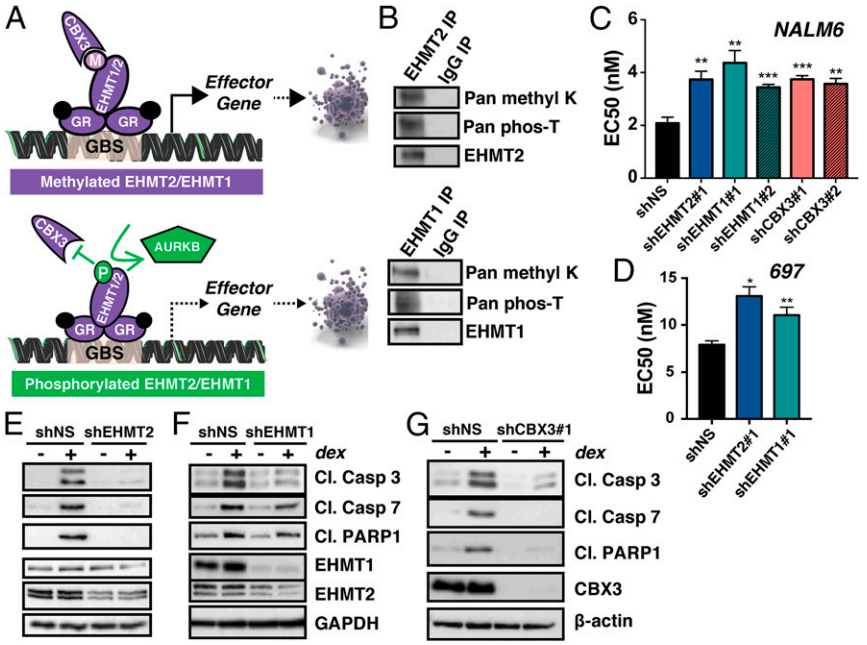

Fig. 3. EHMT2-EHMT1-CBX3 facilitates GC-induced cell death. (*A*) Model for regulation of dex-induced genes involved in B-ALL cell death by GR, EHMT2, EHMT1, CBX3, and AURKB. (*Upper*) GR recruits EHMT2/EHMT1. Methylated EHMT2/EHMT1 recruits CBX3, which recruits RNA polymerase II to activate transcription of cell death genes. (*Lower*) Phosphorylation of EHMT2/EHMT1 by AURKB prevents CBX3 recruitment, reduces death gene activation by GC, and reduces leukemia cell death. (*B*) Methylation and phosphorylation of EHMT2 (*Upper*) and EHMT1 (*Lower*) in NALM6 cells was analyzed by immunoprecipitation (IP) with control IgG or antibody against EHMT2 or EHMT1 followed by immunoblot with indicated antibodies. (*C*) NALM6 cells expressing shEHMT2, shEHMT1, shCBX3, or an shNS were treated with twofold dilutions of dex for 72 h. Cell survival was measured by a fluorescence metabolic assay. EC_{50}, the concentration at which one-half of the cells remain alive, is compared with vehicle controls. Error bars indicate SEM of four independent experiments; P values indicate comparison of each coregulator depletion with shNS using the paired t test. $^{**}P \leq 0.01$; $^{***}P \leq 0.001$. (*D*) Pre-B 697 cells expressing shRNA against EHMT2, EHMT1, or shNS were treated and analyzed as in *C*. $^{*}P \leq 0.05$. (*E*–*G*) NALM6 cells depleted or not for EHMT2 (*E*), EHMT1 (*F*), or CBX3 (*G*) were treated with 100 nM dex (+) or ethanol (–) for 24 h, and indicated proteins were examined by Western blot.

significantly different mRNA levels (Fig. 2 *C*, red dots and *D*, red dots). Most of these genes overlapped with the genes that failed to be properly regulated by dex on coregulator depletion (Fig. 2 *A* and *B*). This analysis revealed that some repressed genes, including *MYC* and *SOX4*, remained aberrantly high and that some potential cell death effector genes were underexpressed on coregulator depletion, including *TSC22D3* (also known as GILZ), *TXNIP*, and *NFKBIA* (36–39) (Dataset S4). Overall, two-thirds of cell death effector genes are no longer significantly regulated by dex on EHMT1/2 depletion in NALM6 cells (Dataset S2: the "NALM6 Effectors" sheet has 18 genes, and the "Misreg EHMT1 or 2 KD Effectors" sheet, which shows the Effector genes that are misregulated by knockdown of EHMT1 or EHMT2, contains 12 of those 18 genes). This abrogation of regulation explains how inhibiting EHMT1/2 could severely blunt sensitivity to dex and shows that the complex is a key driver of dex-induced cell death. In addition, although depletion of EHMT1/2 also attenuates regulation of a similar fraction of buffering genes, the regulation of key buffering genes remains intact. For example, FKBP5, expression of which protects cells against dex-induced cell death, is still strongly up-regulated by dex in EHMT1/2 knockdown. Thus, coregulators have both general and specific effects on the basal and induced expression levels of potential effector genes.

To test whether *TSC22D3*, *TXNIP*, and *NFKBIA* are bona fide effector genes, we measured the effect of shRNA-mediated depletion on GC-induced cell death in NALM6 cells (*SI Appendix*, Fig. S4). For each gene, reduction in expression was accompanied by a significant reduction in sensitivity to dex.

An Intact GR-EHMT1/2-CBX3 Complex Is Required for Full Dex Potency. We previously established the interplay of EHMT1/2, CBX3, and AURKB in A549 cells (16). EHMT1 and EMHT2 directly associate with GR and are automethylated or methylated by each other. Methylation forms a binding interface for CBX3, which is required for full coactivator complex activity when associated with GR. AURKB opposes EHMT1/2 interaction with CBX3 by phosphorylating EHMT1/2, reducing the activity of GR at a subset of genes that require EHMT1/2 (Fig. 3*A*). According to our screen, the depletion of each member of the coregulator complex produced a phenotype that was consistent with its role in dex regulation of cell death effector genes in NALM6 cells [i.e., depletion of GR, EHMT1, EHMT2, and CBX3 was protective against dex, while depletion of AURKB sensitized NALM6 cells to dex (although the AURKB effect was not significant in the screen)] (Fig. 1 *B* and *D*).

To test this model experimentally, we first confirmed that both methylation and phosphorylation on EHMT1/2 were intact in NALM6 cells (Fig. 3*B*). We also confirmed that NALM6 cells depleted of EHMT2, EHMT1, or CBX3 by shRNA were more resistant to dex than controls [nonspecific sequence (shNS)] (Fig. 3*C* and *SI Appendix*, Fig. S5 *A–C*). Another dex-sensitive B-ALL cell line (pre-B 697) also became less sensitive to dex when EHMT2 or EHMT1 was depleted (Fig. 3*D* and *SI Appendix*, Fig. S5*D*), indicating that this mechanism is not limited to the NALM6 cell line. Decreased cleavage of Caspases 3 and 7 and Poly (ADP-Ribose) Polymerase 1 (PARP1) in NALM6 cells depleted of EHMT1/2 or CBX3 after 24 h of dex treatment confirmed attenuation of apoptosis rather than simply growth (Fig. 3 *E–G*).

We next tested whether the coregulator complex was important for regulation of cell death effector genes. Coregulator depletion (Fig. 4*A*) significantly decreased both expression and dex regulation of *TSC22D3*, *TXNIP*, and *NFKBIA* but had no significant effect on dex regulation of *FKBP5*, a gene that did not require EHMT2 or EHMT1 (Fig. 4*B*). To test whether these genes are direct targets of these cofactors, we first validated the GC-induced binding of GR (9) to neighboring response elements using ChIP-qPCR (Fig. 4*C*). Using antibodies to CBX3, we found that it was also recruited to effector gene GR response elements on treatment with dex but not to the GR binding site associated with *FKBP5* (Fig. 4*D*). This indicates that dex induces recruitment of the GR-EHMT1/2-CBX3 complex for full regulation of cell death effector genes, and this mechanism applies only to dex-regulated genes that require EHMT1/2.

Transcriptome Analysis of Paired Diagnostic/Relapsed B-ALL Samples Identifies Genes Associated with Relapse. To test whether alterations in GR cofactor levels contribute to relapse or resistance, we examined patient data. Previously, three studies measured mRNA levels of B-ALL cells from patients at diagnosis and after relapse (GSE3912, GSE18497, GSE28460). Analyzed individually, these studies identified dozens of genes misexpressed on relapse (13–15). A recent metaanalysis of these three studies (40) identified hundreds more, but some misexpressed genes (e.g., *AURKB*) were not identified, and others had surprisingly low-confidence values (e.g., false discovery rate = 0). We, therefore,

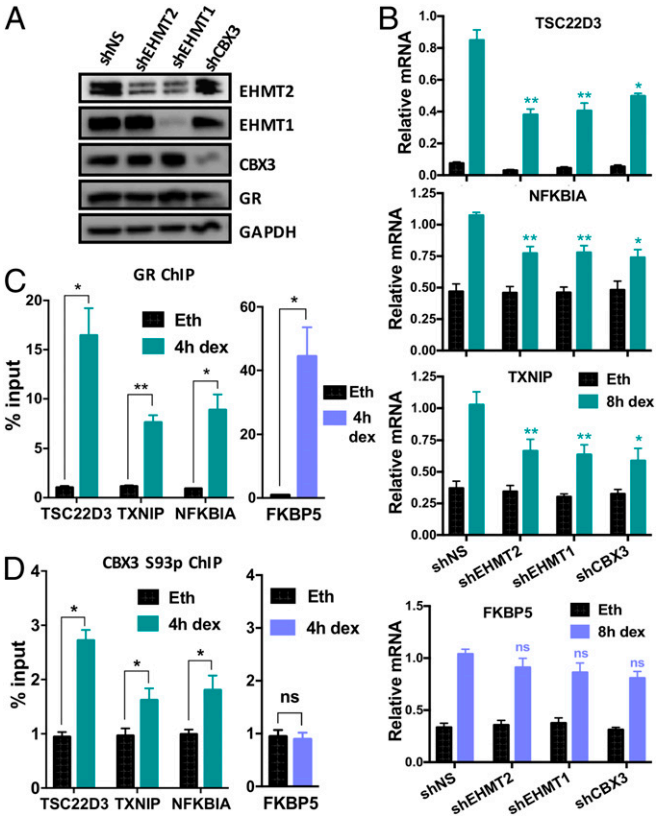

Fig. 4. EHMT2, EHMT1, and CBX3 are coactivators for a subset of GR target genes. (*A*) Immunoblot showing EHMT2, EHMT1, GR, CBX3, and GAPDH protein levels in extracts from NALM6 cells analyzed in *B*. Depletion of EHMT1 resulted in depletion of EHMT2 due to stabilization of EHMT2 protein by EHMT1 protein (16). (*B*) NALM6 cells expressing shRNA against EHMT2, EHMT1, CBX3, or shNS were treated 8 h with 100 nM dex or an equivalent volume of ethanol. mRNA for indicated GR target genes was measured by qRT-PCR and normalized to β-actin mRNA. Results shown are mean ± SEM for three independent experiments. *P* value, paired *t* test comparing each shRNA with shNS. ns, not significant. $*P \leq 0.05$; $**P \leq 0.01$. (*C* and *D*) CBX3 is selectively recruited to EHMT2/EHMT1-dependent GR target genes in response to dex. NALM6 cells were treated with 100 nM dex or ethanol for 4 h. ChIP was performed with antibody against GR (*C*) or CBX3 phosphorylated at S93 (CBX3-S93p) (*D*). Immunoprecipitated DNA was analyzed by qPCR using primers that amplify GR binding regions associated with indicated GR target genes. Results are normalized to input chromatin and shown as mean ± SEM for three independent experiments. *P* value, paired *t* test. ns, not significant. $*P \leq 0.05$; $**P \leq 0.01$.

performed a combined analysis of these datasets to identify genes that are misexpressed on relapse.

Because expression levels were measured on different microarray platforms, we processed each set separately and then combined the results. Arrays were transformed and normalized [*affy* (41), R/Bioconductor], with differentially expressed probes identified by paired analysis [*limma* (42)]. We then combined the *P* values for each gene using the Fisher method. This analysis identified 350 "relapse genes" with expression that was significantly different from diagnostic samples (q value ≤ 0.05). The majority of these (292) were overexpressed (Fig. 5*A*). Using a more relaxed significance cutoff (*P* value ≤ 0.01) for pathway and comparative analyses, we identified 539 top hits, most of which (427) were again overexpressed (Dataset S5).

The results of this combined analysis are consistent with and extend previous analyses. Consistent with previous analyses (43, 44), the top relapse genes were related to cell cycle (e.g., *CCNB2*, *CDK1*) and replication (Fig. 5*B*). However, genes relating to metabolism and nucleotide synthesis were also prevalent. Other relapse genes, such as BIRC5 (Fig. 5*A*), increase cell survival by opposing apoptosis (45). Underexpressed genes were not related to cell cycle but instead, immune cell function (e.g., Toll-like receptor signaling and IL-1 signaling). These data suggest that relapse results from an increase in proliferation and survival and a decrease in immune cell characteristics. Another pathway significantly enriched among relapse genes indicates activation of prostaglandin signaling through PTGER2 (Fig. 5*C*). The significance of this finding suggests a strong link between prostaglandin signaling and relapse that has not been reported previously.

Combining Data from shRNA Screen and Genes Misexpressed at Relapse Identifies Resistance-Relapse Genes. To link misexpression of genes to resistance, we overlapped the top relapse gene hits (Fig. 5*A*) (*P* value ≤ 0.01) with our top hits (*P* value ≤ 0.05) from the shRNA screen for growth (γ) (Fig. 1*A*) or dex sensitivity (ρ) (Fig. 1*B*). About 22% of relapse genes (117) affected growth or survival (*SI Appendix*, Fig. S6*A*). Of these, the genes that contribute to relapse are either overexpressed and decreased growth when depleted or underexpressed and increased growth when depleted (*SI Appendix*, Fig. S6*B*, orange and yellow, respectively). We call the 103 genes that fit these criteria "resistance relapse" genes. These include previously identified cell cycle genes (e.g., *CCNB2*, *CDK1*) (13–15, 40) (Dataset S6 and *SI Appendix*, Fig. S6 *C* and *D*) and newly identified genes, such as *AURKB* (Figs. 1*A* and 5*A*). Both epigenetic (e.g., *DNMT1*, *H2AZ*, *CBX5*, *PRDM2*) and transcription factors (e.g., *PRDM2*, *KLF7*, and *CITED2*) were also identified as resistance relapse genes.

Fewer relapse genes (69 genes) affect GC sensitivity (*SI Appendix*, Fig. S7*A*). Of these, 48 fit the criteria for dex relapse resistance (Dataset S6 and *SI Appendix*, Fig. S7 *B* and *C*). These also include specific cell cycle (*BIRC5*, *CDK1*, and *CCNB2*) and DNA repair (*PARPBP*) genes, the overexpression of which increases resistance to dex (*SI Appendix*, Fig. S7*D*). Each of these represents a potential target for combination therapy with dex. This reveals a previously unrecognized interaction between TOP2A, targeted by anthracyclines (e.g., doxorubicin) in some standard and relapsed therapy, and dex that helps explain their effectiveness in combination.

Surprisingly, few GR coregulators were misexpressed on relapse. Of the 23 coregulators misexpressed (*P* value ≤ 0.01), only 3 (CCNA2, PA2G4, and PSME3) affect dex sensitivity (Dataset S3). Accordingly, few misexpressed coregulators are predicted to interact directly with GR (e.g., SMARCE1). Instead, cell cycle genes, such as CCNA2, CCNE1, and AURKB, are more prevalent and may regulate the activity of GR during the cell cycle. We focused on AURKB, because we had previously shown that it regulates the activity of the EHMT1/2-CBX3 complex (Fig. 3*A*) and was significantly overexpressed at relapse vs. diagnosis (Fig. 5 *A* and *D*), and its overexpression is predicted to enhance growth (*SI Appendix*, Fig. S6*C*), suggesting that it may contribute to relapse.

AURKB Inhibitor Enhances GC Sensitivity of B-ALL Cell Lines and Primary Cells from Patients with Relapsed B-ALL. According to our model, AURKB blunts dex toxicity in B-ALL by phosphorylating EHMT1/2, which interferes with recruitment of CBX3 (Fig. 3*A*). Thus, we hypothesized that inhibition of AURKB would sensitize NALM6 cells to dex by enhancing dex regulation of cell death effector genes. To test this, we used two AURKB-specific inhibitors: ZM447439 (46, 47) and AZD2811 (also known as AZD1152-HQPA) (48–51). Inhibiting AURKB is toxic to NALM6 cells, consistent with our screen data and presumably

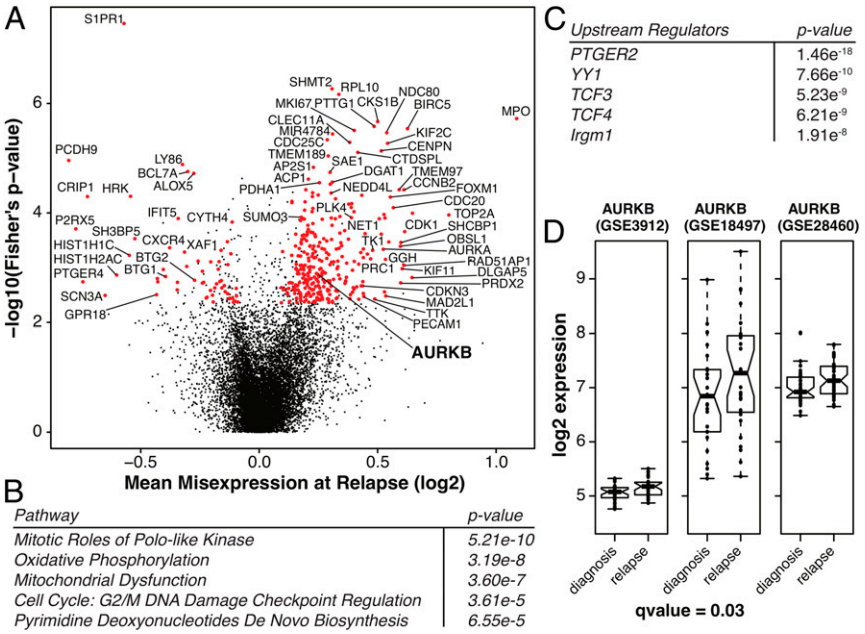

Fig. 5. Genes differentially expressed in B-ALL at relapse vs. diagnosis. (*A*) Three studies collecting paired RNA samples from B-ALL patients at diagnosis and relapse (GSE3912, GSE18497, GSE28460) were combined. A fold change and a *P* value for each gene were first calculated for each dataset. The fold changes were then averaged, and the *P* values were combined using Fisher's method to generate the volcano plot. Genes with a q value ≤ 0.05 are colored red. Outlying genes are labeled. (*B*) Ingenuity pathway analysis of relapse genes indicates that cell cycle genes are highly enriched. (*C*) Upstream analysis of relapse genes shows an enrichment for prostaglandin signaling, specifically through PTGER2. (*D*) AURKB is overexpressed on relapse. Boxplots depict the relative expression of AURKB in B-ALL patient blood samples taken sequentially at diagnosis and relapse for the three different studies. Notches in boxplots represent 95% confidence intervals, with the combined q values shown.

due to cell cycle inhibition (52). Inhibition of AURKB with either ZM447439 or AZD2811 reduced phosphorylation of EHMT2 (*SI Appendix*, Fig. S8 *A* and *B*) and significantly sensitized NALM6 cells to GC-induced cell death (Fig. 6*A*), while inhibition of aurora kinase A (Alisertib) had no effect (*SI Appendix*, Fig. S8*C*). AURKB inhibition by AZD2811 potentiated the apoptotic activity of dex as evidenced by increased cleavage of apoptotic markers in dex-treated NALM6 (Fig. 6*B*). In addition to NALM6 cells, AURKB inhibitors also enhanced the sensitivity of RCH-ACV, a dex-resistant B-ALL cell line (Fig. 6*C*). Importantly, in NALM6 cells, AZD2811 enhanced dex-induced expression of dex effector genes that utilize EHMT2, EHMT1 and CBX3 but not the EHMT2/EHMT1-independent *FKBP5* (Fig. 6*D*). Thus, the effect of the AURKB inhibitor on cell survival involves its selective regulation of EHMT2/EHMT1-dependent GR target genes.

We then tested the combination of AZD2811 and dex in two patient-derived xenograft lines derived from relapsed B-ALL, LAX7R (*KRAS* G12A), and LAX56 [*t(Y;7)(p1.3;p13)*] (53, 54). LAX7R and LAX56 were previously shown to be resistant to both dex and vincristine, another component of standard B-ALL combination chemotherapy. Treatment of these cells with 16 nM AZD2811 alone for 5 d (Fig. 7) reduced cell survival to 70–80% compared with the vehicle-treated control. Treatment with 100–200 nM dex alone reduced survival to 40–60%, whereas lower concentrations of dex had little if any effect on cell survival. In contrast, in combination with 16 nM AZD2811, even 0.1 nM dex reduced cell survival to 10–30%, and lower survival was achieved for LAX56 with higher dex concentrations. Thus, AZD2811 enhanced the dex sensitivity of these two dex-resistant primary B-ALL lines.

Discussion

Elucidating the Mechanism of GC-Induced Cell Death and Identifying Sources of GC Resistance. In B-ALL, treatment resistance arises when cancer cells escape the selective pressure of chemotherapy. However, the routes to relapse are varied and are poorly understood (55). Nonetheless, some common themes have emerged. First, relapse or resistance is correlated with mutations or SNPs in the transcriptional machinery, including transcription factors, such as Ikaros (*IKZF1*), and coregulators, such as *CBP/P300*, *BTG1*, *TBL1XR1* (10, 11, 56), and *NCOA3* (57), and genes involved in nucleotide metabolisms (*NT5C2*) (58). Second, relapse has also been correlated with the misexpression of replication, repair, and cell cycle genes. In our previous work, we used a limited shRNA screen to functionally link cancer, apoptosis, gene expression, and kinase genes to GC sensitivity (9). In this study, we took a comprehensive functional genomics approach by integrating a genome-wide shRNA screen with dex regulation of genes and gene expression data from

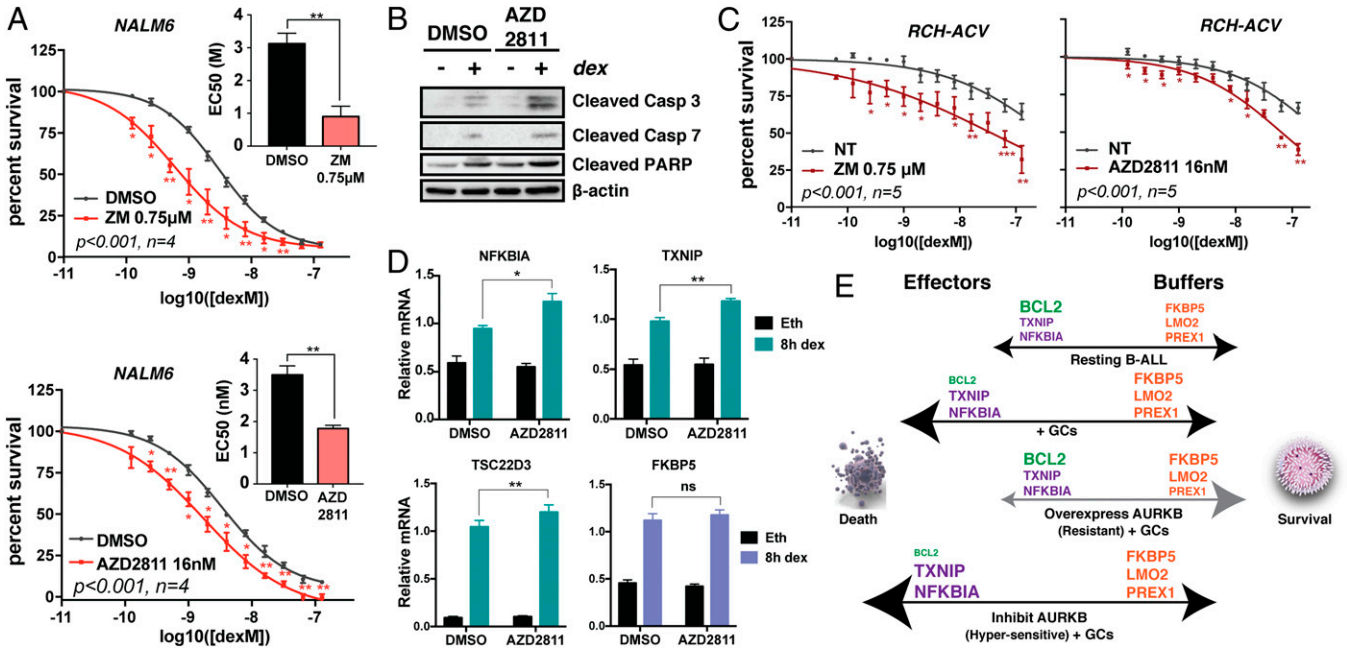

Fig. 6. AURKB inhibitors sensitize NALM6 cells to GC-induced cell death. (*A*) NALM6 cells were treated with indicated dex concentration in addition to 0.75 μM ZM447439 (*Upper*), 16 nM AZD2811 (*Lower*), or equivalent volume of DMSO for 72 h; cell survival was measured by fluorescence metabolic assay. Values measured with dex were normalized to those with ethanol. Percentage of survival, mean ± SEM of four independent experiments; *P* values for individual dex concentrations, paired *t* test. F test comparing the two curves: $P \leq 0.001$. $^{*}P \leq 0.05$; $^{**}P \leq 0.01$. (*Insets*) EC_{50} values, where one-half of the cells remain alive, compared with vehicle controls. Error bars indicate SEM of four independent experiments; *P* values compare AURKB inhibitor treatment with DMSO using paired *t* test. In these graphs, survival of cells treated with aurora kinase inhibitor alone was set to 100%. Samples treated with dex plus kinase inhibitor were normalized to survival observed with kinase inhibitor alone; this more clearly depicts effect of kinase inhibitor on dex sensitivity. $^{**}P \leq 0.01$. (*B*) To NALM6 cells pretreated for 24 h with DMSO or 16 nM AZD2811, ethanol (–) or 100 nM dex (+) was added for an additional 24 h. Indicated proteins were examined by immunoblot. (*C*) RCH-ACV cells were treated with indicated dex concentration in addition to 0.75 μM ZM447439, 16 nM AZD2811, or DMSO for 72 h; cell survival was measured by fluorescence metabolic assay. Normalization was performed as in *A*. Percentage of survival, mean ± SEM of five individual experiments; *P* value for each dex concentration, paired *t* test. F test comparing the two curves: $P \leq 0.001$. $^{*}P \leq 0.05$; $^{**}P \leq 0.01$; $^{***}P \leq 0.001$. (*D*) NALM6 cells pretreated with AZD2811 (16 nM) or DMSO for 24 h were treated for 8 h with 100 nM dex or ethanol. mRNA for indicated GR target genes was measured by qRT-PCR and normalized to β-actin mRNA. Results shown are mean ± SEM for three independent experiments. *P* value, paired *t* test. ns, not significant. $^{*}P \leq 0.05$; $^{**}P \leq 0.01$. (*E*) Model for GC-induced cell death. GC-induced cell death is a balance between effector gene regulation driving cell death and buffer genes that oppose it. Enhanced regulation of effector genes in response to GCs and inhibition of AURKB tip the balance toward cell death. We infer (gray arrows) that overexpression of AURKB attenuates effector gene regulation but retains regulation of some key buffering genes, favoring survival.

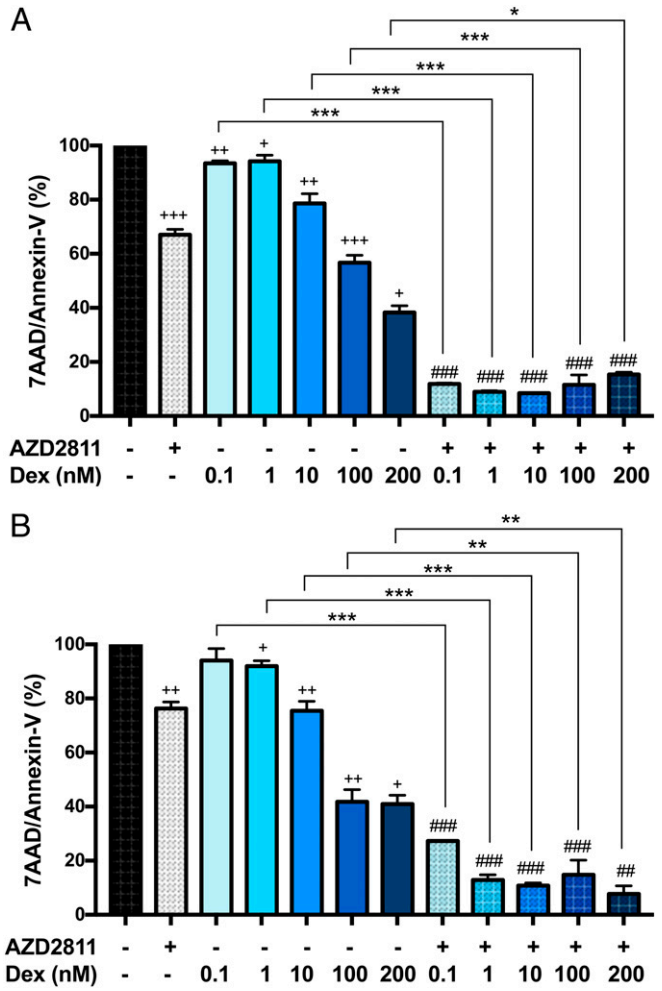

Fig. 7. AURKB inhibitors sensitize primary B-ALL cells from relapsed patients to GC-induced cell death. LAX7R (*A*) or LAX56 (*B*) primary human B-ALL cells were cocultured with OP-9 feeder cells for 5 d in the presence of indicated drugs; cell survival was determined by staining with Annexin/7-AAD. *P* value, a *t* test; different symbols indicate *P* values between different groups. Values are mean ± SD for three biological replicates and are representative of three independent experiments. $^{*}P \leq 0.05$ for significance between combination group and respective dex-treated groups; $^{**}P \leq 0.01$ for significance between combination group and respective dex-treated groups; $^{***}P \leq 0.001$ for significance between combination group and respective dex-treated groups; $^{+}P \leq 0.05$ for significance between dex- or AZD2811 (16 nM)-treated group and DMSO control group;$^{++}P \leq 0.01$ for significance between dex- or AZD2811 (16 nM)-treated group and DMSO control group; $^{+++}P \leq 0.001$ for significance between dex- or AZD2811 (16 nM)-treated group and DMSO control group; $^{\#}P \leq 0.05$ for significance between AZD2811 + dex combination group and AZD2811 group; $^{\#\#}P \leq 0.01$ for significance between AZD2811 + dex combination group and AZD2811 group; $^{\#\#\#}P \leq 0.001$ for significance between AZD2811 + dex combination group and AZD2811 group.

patients to show that misexpression of cell cycle genes can affect GC sensitivity, specifically through the AURKB modification of GR coregulators EHMT1 and EHMT2. Although this is the ultimate focus of this study, data from the shRNA screen and integrated data elucidating how GCs induce cell death and sources of GC resistance on relapse will be invaluable resources for researchers in the leukemia and steroid hormone receptor fields who are looking to functionally validate genes identified through correlative studies, such as SNPs, quantitative trait loci, differential gene expression, and mutational studies.

For example, one attractive pathway for future investigation is prostaglandin signaling. Our screen showed that the GR chaperone *PTGES3* is the second most important protein for GC-induced cell death behind GR (Fig. 1*B*). In addition to serving as a GR chaperone, PTGES3 also converts prostaglandin endoperoxide H2 to prostaglandin E2 (PGE2), which in turn, activates the PTGER2 pathway (31). Analysis of the relapse genes (Ingenuity Pathway Analysis; Qiagen) indicated a strong signature for the presence of PTGER2 signaling (Fig. 5*C*), suggesting that augmenting PTGES3 or administration of PGE2 would likely enhance GC activity in B-ALL. Indeed, PGE2 has been shown to be toxic to B-ALL cells (59, 60). Because PGE2 also protects B-ALL from DNA damage-induced cell death (61, 62), it might be most effective by enhancing dex cytotoxicity in a two-drug combination.

This approach also revealed, surprisingly, that GCs not only induce cell death by regulating effector genes but also, regulate buffering genes that oppose their cytotoxicity. This feature complicates our understanding of GC-induced cell death but also, provides opportunities for potentiation. Take, for example, FKBP5. FKBP5 is strongly up-regulated by dex, but the screen shows that depletion of FKBP5 makes cells more sensitive. This indicates that up-regulation of FKBP5 would protect cells against dex-induced cell death (Fig. 6*E*). Because numerous other genes fall into this category, the mechanism of GC-induced cell death is a balance between regulation of effector genes and buffering genes. If buffering genes are more strongly regulated, GCs will be less potent. However, if effector genes are more strongly regulated, cells are more likely to die.

Our data show that this balance between effectors and buffers is manipulated by AURKB. Although regulation of the majority of effector genes is attenuated by EHMT1/2 depletion and AURKB expression (Dataset S2), regulation of FKBP5 is unchanged (Fig. 6*D*). Thus, the overexpression of AURKB in resistant patients causes resistance by both blunting regulation of effector genes and allowing full regulation of key buffer genes. Conversely, inhibition of AURKB enhances GC cytotoxicity by enhancing regulation of effector genes while leaving FKBP5 regulation unchanged (Fig. 6*E*). Thus, measuring the contribution of each gene to GC-induced cell death helps us understand how overexpression of AURKB, which only affects select genes, is both a potent source of resistance and an excellent target for inhibition.

Enhancing GC Sensitivity of B-ALL by Modulating the Activity of Transcriptional Coregulators. A number of different GR coregulators have been shown to help GR regulate genes in heterologous cell lines in addition to EHMT1/2-CBX3. These include CBP/P300, CARM1, HIC-5, UBC9 (UBE2l), and NCOA2 (33, 63, 64). Of these, only NCOA2 contributed to dex-induced cell death in B-ALL cells. The others either did not affect GC-induced cell death or significantly restrained dex cytotoxicity. Thus, although each of these coregulators might be expected to facilitate GR-induced cell death, our genome-wide shRNA screen delineated which coregulators actually affect GC sensitivity of NALM6 cells, allowing us to focus on EHMT1, EHMT2, and CBX3 (Fig. 1*D*). Based on the screen results, modulating the expression of these and other relevant coregulators would be predicted to enhance GC sensitivity of B-ALL cells. Unfortunately, there is no clear path for achieving this in a clinical setting. A more effective strategy might be to inhibit pathways that impinge on GR coregulator activity, thereby modulating specific biological effects of GC. Indeed, this strategy was born from the finding that, although some GR coregulators and GR itself can be mutated in resistant B-ALL (11), neither the expression level of GR nor its coregulators seem to be associated with resistance. This could be because the GR-independent activity of coregulators in maintaining epigenetic marks and chromatin state is too important to select against, such as reflected in the large number of mRNAs that change in abundance on depletion of EHMT1/2, and concomitant growth impairment. Alternatively, it could be because these coregulators are,

as evidenced by their effect on dex-regulated transcription (Fig. 2), obligate partners of GR in B cells. For example, in our previous work, we showed that GR strongly suppresses B cell development genes (9) and may ultimately be important in B cell specification. As opposed to mutations and posttranslational modifications, which can disrupt specific activities of the proteins, misexpression of GR or its coregulators may be too disruptive to B cells.

The effect of cell cycle genes specifically on GC sensitivity suggested a link between these two pathways. The activity of GR is cell cycle dependent, being most active in G1/S but with reduced activity in G2/M (65, 66). Although CDKs have been shown to modify GR (67, 68), whether this accounts for the cell cycle-dependent activity is not clear. *CDK1* exhibits significantly higher expression levels in relapsed patients and blunts GC activity according to our screen. Inhibitors for CDK1 are under development but are generally not specific, and they have not been as clinically effective as hoped. Also fitting these criteria was AURKB, which we had identified in our previous work as a modulator of GR function through phosphorylation of EHMT1/2 (16). Importantly, the activity of AURKB in regulation of EHMT1/2 seems to be separate from its role promoting cell cycle progression. Because GC regulation of gene expression is greatly reduced during mitosis (65, 66), AURKB regulation of GR activity is likely to be more important during nonmitotic phases of the cell cycle. Ultimately, the enhanced GC-induced cell death by AURKB inhibitors may result from a combination of inhibition of cell cycle progression and the mechanistically separate enhancement of GC-induced expression of EHMT2/EHMT1-dependent GR target genes.

Inhibition of AURKB Sensitizes B-ALL Cells to GC-Induced Cell Death. AURKB, by phosphorylating EHMT1/2, prevents CBX3 binding to EHMT1/2 and CBX3 recruitment on GR binding sites associated with EHMT1/2-dependent genes (Fig. 3*A*) (16). In this manner, AURKB causes a decrease in dex regulation of cell death effector genes while continuing to allow full regulation of some key buffering genes (FKBP5) to strongly inhibit GC-induced cell death. We demonstrate here that modulating regulatory posttranslational modifications of EHMT1/2 rather than their expression (by targeting AURKB catalytic activity) sensitizes B-ALL cells to GC-induced apoptosis (Figs. 6 and 7). Our finding that *AURKB* is significantly overexpressed in patients with relapsed B-ALL (Fig. 5) implicates *AURKB* overexpression as a potential contributor to relapse.

Thus, we define here a role for AURKB in impeding GC-induced cell death through its negative regulation of the GR coactivators EHMT2/EHMT1. The use of AURKB inhibitors to enhance GC efficacy is a potential therapeutic strategy for relapsed B-ALL. Our findings suggest that checking for high levels of *AURKB* at relapse may provide a useful diagnostic test for patients who might respond best to combined treatment with GC and AURKB inhibitor. Although AURKB inhibitors have already been extensively tested as cell cycle-inhibiting agents in clinical trials for some cancers, they have not been tested in combination with GC; thus, our results indicate that additional cell-based and preclinical testing is warranted.

Methods

Cell culture, patient samples, immunoblot, ChIP, and real-time qRT-PCR are described in *SI Appendix, SI Methods*.

Institutional Approval for Patient Samples. Bone marrow and peripheral blood samples from acute lymphoblastic leukemia patients were acquired in compliance with the regulations and approval of the Children's Hospital Los Angeles Institutional Review Board. Informed consent for cell banking was obtained from all human subjects, and all specimens were deidentified before use in this study.

Aggregated Processing of Affymetrix Arrays at Diagnosis and Relapse for Childhood B-ALL. Datasets (GSE3920, GSE18497, GSE28460) (13–15) were downloaded from the Gene Expression Omnibus (https://www.ncbi.nlm.nih.gov/geo/) and imported into R using GEOquery (69). Differential gene expression analysis was performed on each separately (*affy*, *limma*, R/Bioconductor) by paired analysis of samples at diagnosis and relapse (Dataset S5). Average fold changes were calculated, and *P* values from the three datasets were combined by the Fisher method. For each gene, a multiple testing correction was applied by calculating a q value (21). Additional information is provided in *SI Appendix, SI Methods*.

Next Generation shRNA Screen. The shRNA constructs for the next generation knockdown screen were designed and synthesized as previously described (18, 19). The screen was performed largely as described (18) and previously implemented by our group (9). The details and modifications are provided in *SI Appendix, SI Methods*.

Gene Expression Analysis After Coregulator Depletion. NALM6 cells were depleted of either EHMT1 or EHMT2 using lentiviral-delivered shRNAs. Libraries made from total RNA were hybridized to Illumina HT12 v4 gene expression microarrays and processed using R/Bioconductor. Raw intensities were processed using the lumi package (70), and differential expression was tested using limma (42). Additional information is provided in *SI Appendix, SI Methods*. Data is deposited in the Gene Expression Omnibus (71).

Cell Death Assays. Viability of cell lines after dex and AZD2811 treatments was measured with Presto Blue Assay Reagent (Life Technologies). Although treatment with kinase inhibitor alone reduced cell survival (usually by less than 25%), survival for these samples was set to 100%, and samples treated with kinase inhibitor plus dex were normalized to the samples treated with kinase inhibitor alone; this data treatment shows more clearly the effect of the kinase inhibitor on dex sensitivity of the cells.

For patient samples, apoptosis from treatment was assessed using the PE Annexin V Apoptosis Detection Kit with 7-AAD.

ACKNOWLEDGMENTS. This work was supported by NIH Grants R01CA172896 (to Y.-M.K.), R37DK055274 (to M.R.S.), and R01DK043093 (to M.R.S.) and NIH Cancer Center Support Grant P30CA014089 (to the University of Southern California Norris Comprehensive Cancer Center, which supported the Molecular and Cell Biology Core Facilities used in this project). M.A.P. was supported by NIH/National Cancer Institute (NCI) Grant K99/R00CA149088, Roy J. Carver Charitable Trust Grant 01-224, the American Cancer Society Institutional Research Grant Program, and Holden Comprehensive Cancer Center NIH/NCI Grant P30CA086862. M.K. was supported by NIH/NCI Grant K99/R00 CA181494 and a Stand Up to Cancer Innovative Research Grant.

1. PDQ Pediatric Treatment Editorial Board (2002) *Childhood Acute Lymphoblastic Leukemia Treatment (PDQ): Health Professional Version* (PDQ) (National Cancer Institute, Bethesda).
2. Dördelmann M, et al. (1999) Prednisone response is the strongest predictor of treatment outcome in infant acute lymphoblastic leukemia. *Blood* 94:1209–1217.
3. Cario G, et al. (2008) Initial leukemic gene expression profiles of patients with poor in vivo prednisone response are similar to those of blasts persisting under prednisone treatment in childhood acute lymphoblastic leukemia. *Ann Hematol* 87:709–716.
4. Lönnerholm G, et al. (2009) In vitro cellular drug sensitivity at diagnosis is correlated to minimal residual disease at end of induction therapy in childhood acute lymphoblastic leukemia. *Leuk Res* 33:46–53.
5. Yamamoto KR (1985) Steroid receptor regulated transcription of specific genes and gene networks. *Annu Rev Genet* 19:209–252.
6. Smith LK, Cidlowski JA (2010) Glucocorticoid-induced apoptosis of healthy and malignant lymphocytes. *Prog Brain Res* 182:1–30.
7. Terwilliger T, Abdul-Hay M (2017) Acute lymphoblastic leukemia: A comprehensive review and 2017 update. *Blood Cancer J* 7:e577.
8. Park JH, et al. (2018) Long-term follow-up of CD19 CAR therapy in acute lymphoblastic leukemia. *N Engl J Med* 378:449–459.
9. Kruth KA, et al. (2017) Suppression of B-cell development genes is key to glucocorticoid efficacy in treatment of acute lymphoblastic leukemia. *Blood* 129:3000–3008.
10. Jones CL, et al. (2014) Loss of TBL1XR1 disrupts glucocorticoid receptor recruitment to chromatin and results in glucocorticoid resistance in a B-lymphoblastic leukemia model. *J Biol Chem* 289:20502–20515.
11. Mullighan CG, et al. (2011) CREBBP mutations in relapsed acute lymphoblastic leukaemia. *Nature* 471:235–239.
12. Madhusoodhan PP, Carroll WL, Bhatla T (2016) Progress and prospects in pediatric leukemia. *Curr Probl Pediatr Adolesc Health Care* 46:229–241.
13. Bhojwani D, et al. (2006) Biologic pathways associated with relapse in childhood acute lymphoblastic leukemia: A Children's Oncology Group study. *Blood* 108:711–717.
14. Hogan LE, et al. (2011) Integrated genomic analysis of relapsed childhood acute lymphoblastic leukemia reveals therapeutic strategies. *Blood* 118:5218–5226.
15. Staal FJT, et al. (2010) Genome-wide expression analysis of paired diagnosis-relapse samples in ALL indicates involvement of pathways related to DNA replication, cell cycle and DNA repair, independent of immune phenotype. *Leukemia* 24:491–499.
16. Poulard C, et al. (2017) A post-translational modification switch controls coactivator function of histone methyltransferases G9a and GLP. *EMBO Rep* 18:1442–1459.

17. Kampmann M, et al. (2015) Next-generation libraries for robust RNA interference-based genome-wide screens. *Proc Natl Acad Sci USA* 112:E3384–E3391.
18. Kampmann M, Bassik MC, Weissman JS (2014) Functional genomics platform for pooled screening and generation of mammalian genetic interaction maps. *Nat Protoc* 9:1825–1847.
19. Kampmann M, Bassik MC, Weissman JS (2013) Integrated platform for genome-wide screening and construction of high-density genetic interaction maps in mammalian cells. *Proc Natl Acad Sci USA* 110:E2317–E2326.
20. Bassik MC, et al. (2013) A systematic mammalian genetic interaction map reveals pathways underlying ricin susceptibility. *Cell* 152:909–922.
21. Storey JD, Tibshirani R (2003) Statistical significance for genomewide studies. *Proc Natl Acad Sci USA* 100:9440–9445.
22. Bolouri H, et al. (2018) The molecular landscape of pediatric acute myeloid leukemia reveals recurrent structural alterations and age-specific mutational interactions. *Nat Med* 24:103–112.
23. Chen S, et al. (2011) Novel non-TCR chromosome translocations t(3;11)(q25;p13) and t(X;11)(q25;p13) activating LMO2 by juxtaposition with MBNL1 and STAG2. *Leukemia* 25:1632–1635.
24. Yan L, et al. (2012) Clinical, immunophenotypic, cytogenetic, and molecular genetic features in 117 adult patients with mixed-phenotype acute leukemia defined by WHO-2008 classification. *Haematologica* 97:1708–1712.
25. Eldridge AG, Li Y, Sharp PA, Blencowe BJ (1999) The SRm160/300 splicing coactivator is required for exon-enhancer function. *Proc Natl Acad Sci USA* 96:6125–6130.
26. Wang T, et al. (2017) Gene essentiality profiling reveals gene networks and synthetic lethal interactions with oncogenic ras. *Cell* 168:890–903.e15.
27. Rahman S, et al. (2017) Activation of the *LMO2* oncogene through a somatically acquired neomorphic promoter in T-cell acute lymphoblastic leukemia. *Blood* 129:3221–3226.
28. Bakker E, et al. (2017) Insight into glucocorticoid receptor signalling through interactome model analysis. *PLoS Comput Biol* 13:e1005825–e1005826.
29. Kininis M, Kraus WL (2008) A global view of transcriptional regulation by nuclear receptors: Gene expression, factor localization, and DNA sequence analysis. *Nucl Recept Signal* 6:e005.
30. Petta I, et al. (2016) The interactome of the glucocorticoid receptor and its influence on the actions of glucocorticoids in combatting inflammatory and infectious diseases. *Microbiol Mol Biol Rev* 80:495–522.
31. Tanioka T, Nakatani Y, Semmyo N, Murakami M, Kudo I (2000) Molecular identification of cytosolic prostaglandin E2 synthase that is functionally coupled with cyclooxygenase-1 in immediate prostaglandin E2 biosynthesis. *J Biol Chem* 275:32775–32782.
32. Lai AY, Wade PA (2011) Cancer biology and NuRD: A multifaceted chromatin remodelling complex. *Nat Rev Cancer* 11:588–596.
33. Bittencourt D, et al. (2012) G9a functions as a molecular scaffold for assembly of transcriptional coactivators on a subset of glucocorticoid receptor target genes. *Proc Natl Acad Sci USA* 109:19673–19678.
34. Lee DY, Northrop JP, Kuo M-H, Stallcup MR (2006) Histone H3 lysine 9 methyltransferase G9a is a transcriptional coactivator for nuclear receptors. *J Biol Chem* 281:8476–8485.
35. Tachibana M, et al. (2005) Histone methyltransferases G9a and GLP form heteromeric complexes and are both crucial for methylation of euchromatin at H3-K9. *Genes Dev* 19:815–826.
36. Bruscoli S, et al. (2015) Lack of glucocorticoid-induced leucine zipper (GILZ) deregulates B-cell survival and results in B-cell lymphocytosis in mice. *Blood* 126:1790–1801.
37. Chen Z, et al. (2011) Thioredoxin-binding protein-2 (TBP-2/VDUP1/TXNIP) regulates T-cell sensitivity to glucocorticoid during HTLV-I-induced transformation. *Leukemia* 25:440–448.
38. Fuchs O (2010) Transcription factor NF-κB inhibitors as single therapeutic agents or in combination with classical chemotherapeutic agents for the treatment of hematologic malignancies. *Curr Mol Pharmacol* 3:98–122.
39. Schmidt S, et al. (2004) Glucocorticoid-induced apoptosis and glucocorticoid resistance: Molecular mechanisms and clinical relevance. *Cell Death Differ* 11:S45–S55.
40. Chow Y-P, Alias H, Jamal R (2017) Meta-analysis of gene expression in relapsed childhood B-acute lymphoblastic leukemia. *BMC Cancer* 17:120.
41. Gautier L, Cope L, Bolstad BM, Irizarry RA (2004) affy–Analysis of Affymetrix GeneChip data at the probe level. *Bioinformatics* 20:307–315.
42. Ritchie ME, et al. (2015) limma powers differential expression analyses for RNA-sequencing and microarray studies. *Nucleic Acids Res* 43:e47.
43. McDonald ER, 3rd, et al. (2017) Project DRIVE: A compendium of cancer dependencies and synthetic lethal relationships uncovered by large-scale, deep RNAi screening. *Cell* 170:577–592.e10.
44. Rodriguez-Fraticelli AE, et al. (2018) Clonal analysis of lineage fate in native haematopoiesis. *Nature* 553:212–216.
45. Fulda S (2009) Inhibitor of apoptosis proteins in hematological malignancies. *Leukemia* 23:467–476.
46. Ditchfield C, et al. (2003) Aurora B couples chromosome alignment with anaphase by targeting BubR1, Mad2, and Cenp-E to kinetochores. *J Cell Biol* 161:267–280.
47. Girdler F, et al. (2006) Validating Aurora B as an anti-cancer drug target. *J Cell Sci* 119:3664–3675.
48. Mortlock AA, et al. (2007) Discovery, synthesis, and in vivo activity of a new class of pyrazoloquinazolines as selective inhibitors of aurora B kinase. *J Med Chem* 50:2213–2224.
49. Wilkinson RW, et al. (2007) AZD1152, a selective inhibitor of Aurora B kinase, inhibits human tumor xenograft growth by inducing apoptosis. *Clin Cancer Res* 13:3682–3688.
50. Ashton S, et al. (2016) Aurora kinase inhibitor nanoparticles target tumors with favorable therapeutic index in vivo. *Sci Transl Med* 8:325ra17.
51. Floc'h N, et al. (2017) Optimizing therapeutic effect of aurora B inhibition in acute myeloid leukemia with AZD2811 nanoparticles. *Mol Cancer Ther* 16:1031–1040.
52. Goldenson B, Crispino JD (2015) The aurora kinases in cell cycle and leukemia. *Oncogene* 34:537–545.
53. Park E, et al. (2011) Targeting survivin overcomes drug resistance in acute lymphoblastic leukemia. *Blood* 118:2191–2199.
54. Adam E, et al. (2017) The PI3Kδ inhibitor idelalisib inhibits homing in an in vitro and in vivo model of B ALL. *Cancers (Basel)* 9:121.
55. Bhojwani D, et al. (2017) Investigating the biology of relapsed acute leukemia: Proceedings of the therapeutic advances for childhood leukemia & lymphoma (TACL) consortium biology working group. *Pediatr Hematol Oncol* 34:355–364.
56. van Galen JC, et al. (2010) BTG1 regulates glucocorticoid receptor autoinduction in acute lymphoblastic leukemia. *Blood* 115:4810–4819.
57. Yang JJ, et al. (2009) Genome-wide interrogation of germline genetic variation associated with treatment response in childhood acute lymphoblastic leukemia. *JAMA* 301:393–403.
58. Meyer JA, et al. (2013) Relapse-specific mutations in NT5C2 in childhood acute lymphoblastic leukemia. *Nat Genet* 45:290–294.
59. Giordano L, et al. (1997) Growth inhibition of B-cell precursor acute lymphoblastic leukemia cell lines by monocytes: A role for prostaglandin E2. *Leuk Res* 21:925–932.
60. Soleymani Fard S, Jeddi Tehrani M, Ardekani AM (2012) Prostaglandin E2 induces growth inhibition, apoptosis and differentiation in T and B cell-derived acute lymphoblastic leukemia cell lines (CCRF-CEM and Nalm-6). *Prostaglandins Leukot Essent Fatty Acids* 87:17–24.
61. Naderi EH, et al. (2015) Bone marrow stroma-derived PGE2 protects BCP-ALL cells from DNA damage-induced p53 accumulation and cell death. *Mol Cancer* 14:14–12.
62. Naderi EH, et al. (2013) Selective inhibition of cell death in malignant vs normal B-cell precursors: Implications for cAMP in development and treatment of BCP-ALL. *Blood* 121:1805–1813.
63. Cho S, Kagan BL, Blackford JA, Jr, Szapary D, Simons SS, Jr (2005) Glucocorticoid receptor ligand binding domain is sufficient for the modulation of glucocorticoid induction properties by homologous receptors, coactivator transcription intermediary factor 2, and Ubc9. *Mol Endocrinol* 19:290–311.
64. Chodankar R, Wu D-Y, Schiller BJ, Yamamoto KR, Stallcup MR (2014) Hic-5 is a transcription coregulator that acts before and/or after glucocorticoid receptor genome occupancy in a gene-selective manner. *Proc Natl Acad Sci USA* 111:4007–4012.
65. Hsu SC, Qi M, DeFranco DB (1992) Cell cycle regulation of glucocorticoid receptor function. *EMBO J* 11:3457–3468.
66. Hsu SC, DeFranco DB (1995) Selectivity of cell cycle regulation of glucocorticoid receptor function. *J Biol Chem* 270:3359–3364.
67. Krstic MD, Rogatsky I, Yamamoto KR, Garabedian MJ (1997) Mitogen-activated and cyclin-dependent protein kinases selectively and differentially modulate transcriptional enhancement by the glucocorticoid receptor. *Mol Cell Biol* 17:3947–3954.
68. Kumar R, Calhoun WJ (2008) Differential regulation of the transcriptional activity of the glucocorticoid receptor through site-specific phosphorylation. *Biologics* 2:845–854.
69. Davis S, Meltzer PS (2007) GEOquery: A bridge between the Gene Expression Omnibus (GEO) and BioConductor. *Bioinformatics* 23:1846–1847.
70. Du P, Kibbe WA, Lin SM (2008) lumi: a pipeline for processing Illumina microarray. *Bioinformatics* 24:1547–1548.
71. Pufall MA, Fang M, Shelton D (2018) Analysis of the effect of cofactor knockdown on dexamethasone-induced gene expression in B-cell acute lymphoblastic leukemia. Gene Expression Omnibus. Available at https://www.ncbi.nlm.nih.gov/geo/query/acc.cgi?acc=GSE118992. Deposited August 28, 2018.